Techno-Economic Analysis of a Solar Hybrid Combined Cycle Power Plant Integrated with a Packed Bed Storage at Gas Turbine Exhaust

Silvia Trevisan^{1, a)}, Rosa P. Merchán^{2, 3, b)}, Rafael Guédez¹, María J. Santos^{2, 3}, Alejandro Medina^{2, 3}, Björn Laumert¹, Antonio Calvo-Hernández^{2, 3}

¹Department of Energy Technology, KTH Royal Institute of Technology, 100 44 Stockholm, Sweden. ²Department of Applied Physics, University of Salamanca, 37008 Salamanca, Spain. ³IUFFYM, University of Salamanca, 37008 Salamanca, Spain.

> ^{a)} Corresponding author: <u>trevisan@kth.se</u> ^{b)} <u>rpmerchan@usal.es</u>

Abstract. The present work performs a techno-economic analysis of an innovative solar-hybrid combined cycle composed of a topping gas turbine coupled to a bottoming packed bed thermal energy storage at the gas turbine exhaust, which runs in parallel to a bottoming steam cycle. Plant performances have been evaluated in terms of the capacity factor, the specific CO₂ emissions, the capital expenditure, and the Levelised Cost of Electricity. The influence of the combustion chamber outlet temperature, solar multiple and energy storage capacity has been assessed by means of a sensitivity analysis. The present study also compares the previously listed performance against that of conventional molten salt tower Concentrating Solar Power plants and traditional combined cycle gas turbine power plants with equivalent installed capacities and load factors. The results show that it is worth hybridizing the system, particularly at high combustion chamber outlet temperature, large storage size and solar multiple. Furthermore, plant configurations leading to a Levelised Cost of Electricity lower than 110 \$/MWh can be achieved for a capacity factor of about 60%. Under these working conditions, the proposed configuration would be only 1.66 times more costly than an equivalent size CCGT. At the same time, it would yield less than half of the emissions of the latter. Simultaneously, the proposed layout is considerably cheaper than an equivalent molten salt Concentrating Solar Power plant.

INTRODUCTION

The introduction of more advanced power cycles with higher conversion efficiencies has been identified as one of the key alternatives for enhancing the economic viability, and the flexibility, of Concentrated Solar Power (CSP) plants. This paper performs a techno-economic assessment of an innovative solar-hybrid combined cycle composed of a topping solar-hybrid gas turbine (GT) coupled to a bottoming packed bed TES at the GT exhaust, which runs in parallel also to a traditional bottoming steam cycle. The plant layout itself is shown in Fig. 1 and is similar to the Sunspot cycle introduced by Harper et al. [1], but in this study the focus is placed on larger installed capacities (300MWe instead of 120MWe). Furthermore, a sensitivity analysis of key design variables such as the temperature at the outlet of the combustion chamber (TCC), the Thermal Energy Storage (TES) size, the Solar Multiple (SM), and the nominal power ratio between the gas and steam cycle (γ) is performed. In this first assessment, the selected indicators for evaluating the performance have been the Levelized Cost of Electricity (LCoE), the specific CO₂ emissions, the Capacity Factor (CF), net electrical energy produced and the thermal wasted energy. The study also compares such performance against that of conventional molten salt tower CSP plants (STCSP) and traditional combined cycle gas turbine (CCGT) power plants with equivalent installed capacities and load factors. As expected, it is shown that despite being more costly than conventional CCGTs, and less environmentally friendly than purely solar driven tower CSP plants, best configurations of the proposed layout can result in an attractive compromise of

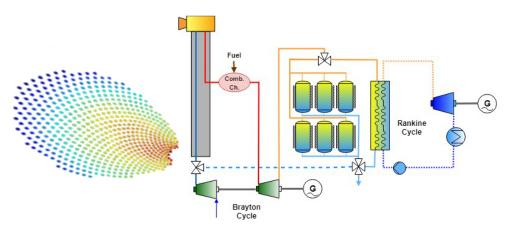


FIGURE 1. Scheme of the studied hybrid solar combined cycle plant.

both. Ultimately, the authors consider that the value of decoupling the topping and bottoming cycles through an intermediate TES would be more appreciated in techno-economic optimization studies coupled to TES dispatch optimization algorithms under hourly price variations or load profile demands. The flexibility of the proposed layout is expected to lead to attractive solutions for flexible energy generation at a reduced environmental cost, ahead of equivalent STCSPs or CCGTs plants. This work intends to be a stepping stone in such comparative analysis. Although it is focused towards a stable electricity production during the central hours of the day and a baseline smaller production during the rest of the day, results could be extrapolated to other particular dispatch objectives.

SYSTEM CONFIGURATION

The present work introduces a 300 MWe solar-hybrid combined cycle composed of a topping solar-hybrid gas turbine (GT) coupled to a traditional bottoming steam cycle and a packed bed TES at the GT exhaust. The plant scheme is shown in Fig.1. During the day, when the incoming solar radiation is higher than a minimum value, the air entering the system at ambient conditions is compressed up to 15 bar in the Brayton cycle compressor and heated up to 800°C in the receiver (REC). As Direct Normal Irradiance (DNI) changes in each time step, GT mass flow in the receiver varies accordingly in order to reach that 800°C temperature. To fully exploit the Brayton cycle, the air temperature is raised by means of a combustion chamber up to 1200°C, design GT inlet temperature. The air is then expanded in the GT and exits at approximately 580°C and ambient pressure. At GT exhaust, the air is partially sent to the heat recovery steam generator (HRSG), where superheated steam is produced (at nominal load conditions), and to a parallel set of packed bed TES units where heat is stored in order to extend the bottoming cycle production after sun hours or during cloudy periods. Therefore, during night time, air is ventilated through the TES unit and then sent to the HRSG where superheated steam is generated. Hence, ST mass flow is kept constant when DNI is higher than the minimum value and it slowly decreases during discharge of TES.

Control Logic

In order to operate the CSP plant, a control logic has been built considering a deterministic operating regime, also identified as one of the limitations to further investigate by means of introducing a dispatch optimizer in a subsequent study. Thus, the control of the plant has been designed such as to allow the GT to produce whenever there is enough energy from the solar field, and to let the bottoming cycle operate continuously – as long as there is energy in the TES. Depending on the actual Direct Normal Irradiance (DNI) and TES State of the Charge (SoC), evaluated at each time step, five different operation modes (OMs) can be identified. The control logic associated flow chart is shown in Fig. 2, while Table 1 defines the main implications of each operational mode in the plant control. During daylight, when the solar input alone is sufficiently high to cover the steam cycle design heat load ($DNI > DNI_{min_{ST}}$), the GT runs at a load that mirrors the DNI trend. Furthermore, if the TES SoC is lower than SoC_{max}, the mass flow at GT outlet is divided into two streams: one constant mass flow performs the Rankine cycle at on-design conditions; meanwhile, the other one, which inherits the time variation, charges the TES (OM1). If the TES units are already full, the excess of thermal power at the GT outlet is wasted and the Steam Turbine (ST) continues working at design conditions (OM2).

On the other side, when the solar input is not sufficient for running the ST, the TES units are discharged extending the CSP plant power production as long as the SoC remains above a minimum level (SOC_{min}). Specifically, the design air stream goes through the TES increasing its temperature and, then, it performs the Rankine cycle at off-design conditions since the TES outflow temperature and consequently the ST inlet temperature decreases as the storage units are being discharged (OM3). When SoC falls below the minimum level, TES is considered as empty, so there is no power production at all (OM4). It can also occur that during the early mornings the DNI is lower than the minimum threshold and the TES empty, in such a situation the GT works a low partial load from solar energy, while the ST is still shut off as the solar irradiance is not high enough for its ST start-up (OM 5). Instead, when a similar DNI pattern occurs during the late evening, with the TES at least partially charged, OM3 is preferred in order to operate the ST and limits the GT operation at low load conditions. The whole control strategy has been implemented together with plant layout in TRNSYS® software with the objective of performing dynamic simulations, as it is explained in Methodology section.

TAI	BLE 1. (Dperational Modes (Ol CSP plant con	,	nplications in	DNI,=0?	0 <dni,t< DNImin?</dni,t<
OM	GT	ST	REC	TES	YES	YES
1	ON	ON: Design	ON	Charge	OM 4 SoC,t-1 > YES SoCmin? O	M 3 SoC,t-1 SoCmin?
2	ON	ON: Design	ON	Full	OWI 4 SoCmin?	SoCmin?
3	OFF	ON: Off-Design	OFF	Discharge	Ĩ. Internet in the second s	YES
4	OFF	OFF	OFF	Empty		OM 5 SoC,t-1
5	ON	OFF	ON	Empty		
	•					a 1 0.1

FIGURE 2. Control strategy flowchart of the proposed layout

DNI +

Economic Model

In the present work the capital investment (CAPEX) and the LCoE have been chosen as the main economic indicators in order to measure both the investment and the relative profitability of the studied hybrid CSP plant. The CAPEX has been calculated by adding the direct cost for all the main specific components (Brayton and Rankine cycle turbomachinery, combustion chamber, HRSG, condenser, electrical generators, heliostat field and land, tower, receiver, TES, and auxiliaries) and indirect cost (engineering, procurement and construction, taxes and decommissioning). The cost of the Brayton and Rankine cycle components and relative auxiliaries have been calculated according to the scaling function presented in [2]. In order to consider the effects of inflation, all scaling functions have been multiplied by the ratio between the reference Marshall & Swift index for 2018 and the one for the year of the publication when the cost function was proposed, $f_{infl}^{ref} = M\&S_{2018}/M\&S_{ref}$. The reference Marshall & Swift indexes have been gathered from [3]. The cost for the heliostat field has been evaluated by means of the cost functions proposed in [4], while the tower cost has been calculated based on the functions proposed in [2]. The air receiver cost (C_{REC}) has been based on the values proposed by Schwarzbözl *et al.* [5], the specific costs suggested for low, medium and high temperature receiver have been linearly fitted obtaining Eq. (1), where A_{REC} and T_{REC} account for the receiver area and temperature, respectively.

$$C_{REC} = f_{infl}^{2006} \left[A_{REC}[m^2] \left(79 \left[\frac{USD}{m^{2} °C} \right] T_{REC}[°C] - 20833 \left[\frac{USD}{m^2} \right] \right) \right]$$
(1)

A more detailed approach has been followed to evaluate the cost of the storage units. Indeed, the overall TES cost has been calculated by adding the cost of the filler material (natural rocks), high and low temperature insulation, TES tank main material (MA253 Steel) and foundation accordingly to the specific prices reported in Table 2. The remaining cost components have been evaluated thanks to the data and approach presented in [2].

TABLE 2. Specific costs of TES main components.					
Rocks $[\%/m^3]$	66				
High Temperature Insulation [\$/m ³]	4'269				
Low Temperature Insulation [\$/m ³]	616				
MA253 Steel $[\%/m^3]$	42'354				
Foundation [\$/m ²]	1'210				

Furthermore, the operational cost (OPEX) has been evaluated including the cost of required fuel assumed as natural gas (NG), CO₂ emissions, O&M, contracts and administration. For the NG, a fixed price has been assumed, equal to 0.142 \$/kg_{NG}; while for the CO₂ emissions an allowance of 0.0284 \$/kg_{CO2} has been considered. Finally, the LCoE is calculated by means of Eq. (2) as function of the annualized CAPEX and decommissioning cost, annual OPEX and net annual energy production E_{NET} . The initial investment, CAPEX, and the decommissioning cost, C_{Decom} , are translated into equivalent annual payments thanks to the two factors α and β , which are defined in Eq. (3) and (4), where *i* is the real debt interest rate, k_{ins} is the annual insurance rate, assumed equal to 7% and 1% respectively. While, n_{op} is the plant lifetime, n_{con} is the plant construction time and n_{cdec} is the plant decommissioning time, equal to 30, 2 and 2 years respectively.

$$LCoE = \frac{\alpha \cdot CAPEX + \beta \cdot C_{Decom} + OPEX}{E_{NFT}}$$
(2)

$$\alpha = \frac{(1+i)^{n_{con}} - 1}{\binom{n_{con} \cdot i}{(1+i)^{n_{op}} - 1}} + k_{ins}$$
(3)

$$\beta = \frac{(1+i)^{n_{dec}} - 1}{n_{dec} \cdot i(1+i)^{n_{dec}-1}} \cdot \frac{i}{(1+i)^{n_{op}} - 1}$$
(4)

METHODOLOGY

In order to study the thermo-economic performance of the proposed hybrid CSP plant, different interconnected models have been built:

- A steady state thermodynamic CSP plant model to evaluate design working conditions and some design input value for the different components

- A System Advisor Model (SAM) model for simulating the heliostats solar field and for obtaining the solar field efficiency matrixes at different SM

- A transient TRNSYS model, with integrated control logic and meteorological data gathered from Meteonorm database, where annual simulations have been performed

- An economic model, in MatLab scripts, to evaluate all costs functions and overall plant Key Performance Indicators (KPIs)

At last, sensitivity analysis with regards to the desired outlet temperature from the combustion chamber (TCC), the TES size, the SM, and the nominal power ratio between the gas and steam cycle (γ) were performed. This last power ratio is defined just as the proportion of GT power (P_{GT}) over ST power (P_{ST}) at design: $\gamma = \frac{P_{GT}}{P_{ST}}$. Besides the LCoE, other indicators considered were the specific emissions, the net energy production, the wasted or defocused energy and the capacity factor (CF), evaluated as in Eq. (5), where h_{TES} corresponds to the TES size (in number of hours).

$$CF = \frac{E_{NET}}{[P_{GT} \cdot (24 - h_{TES}) + P_{ST} \cdot 24] \cdot 365}$$
(5)

The previously listed four input parameters were considered because they constitute the most interesting and valuable variables for the sensitivity analysis. Outlet temperature of the combustion chamber was chosen for the sensitivity analysis since it establishes inlet gas turbine temperature (so, Brayton efficiency) and also since it is directly related to the hybridization level of the plant, namely to the fuel consumption. Therefore, this parameter will be crucial for trade-off between lower hybridization level and higher efficiency. Furthermore, TES size refers to the amount of stored energy, which is one of the two heat sources for Rankine cycle. Thus, it turns out to be critical for steam turbine production and therefore to enhance the capacity factor and extend the production during night-time. The third analyzed parameter is the Solar Multiple (SM), associated with solar field size, which is decisive for the design of the plant since it determines the heliostat field size, so the collected power in the receiver and consequently the receiver air mass flow. Finally, gas turbine to steam turbine power ratio (γ) is studied, provided that total design power remains the same. The effect of this ratio is related to both design GT and ST mass flows. For the sensitivity analysis, the four aforementioned parameters were varied up and down around the base case values in the parameters ranges collected at Table 3. TCC is fixed at 1200°C for the base case. Solar receiver heats up air mass flow up to 800°C, so 800°C was also chosen as lower limit value for TCC with the purpose of reproducing plant behavior in pure solar mode, without combustion chamber necessity. The Gas Turbine to Steam Turbine power ratio (γ) is only computed for two values

around the base case for preserving feasible and realistic values while presenting significant effects on output variables.

Parameters	TCC	TES size	SM	γ
Base case	1200 °C	8 h	1.5	5
Range	800 °C − 1400 °C	4 h - 12 h	1 - 2	3 - 9
Step	100 °C	2 h	0.25	-

TABLE 3. Parameters ranges for the sensitivity analysis.

RESULTS AND DISCUSSION

CSP Plant Performance – Design Case

The studied CSP plant was located in Seville, Spain (37.39° N, - 5.99° E). The evolution of main results with time is plotted for the base case as an example for the first of July in Fig. 3. Where GT and ST power represent the net electrical power produced; while the thermal wasted power is the sum of the power wasted at the TES outlet during OM1, the curtailed one during OM5 and the remaining power at the economizer hot side outlet during OM1, OM2 and OM3. GT is only working when DNI is higher than the minimum value (OM 1 and OM 2), as it was imposed in TRNSYS logic control. Nevertheless, ST is also producing electricity when Sun goes down, extending number of generating hours and so the capacity factor. During the initial hours of the day, plant is stopped (OM4), until DNI is higher than the minimum value, when OM 1 starts. Afterwards, if TES is full, OM 2 is established and, finally, when DNI becomes zero again, plant is under OM 3. There is an intermediate state between OM 4 and OM 1, when ST has not started to run, which is denominated OM 5. SOC is always between 0.1 and 0.95, it is never allowed to reach 0 or 1 for stability reasons. The emission of CO₂ is higher around central hours of the day, when DNI is maximum, since the associated air mass flow is higher and, so, the fuel consumption. It is worth noting that during the second part of

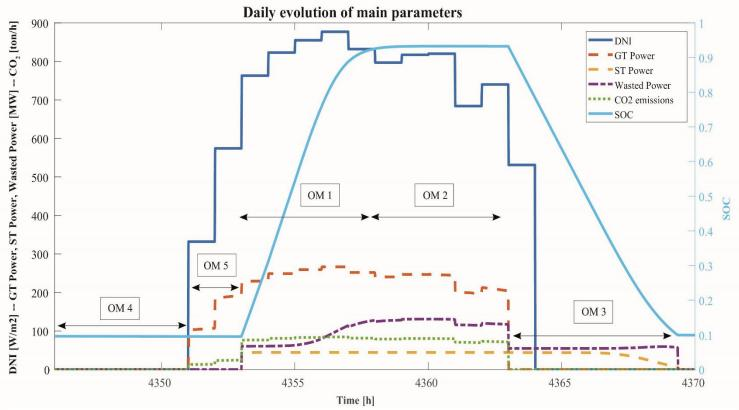


FIGURE 3. Daily evolution of main variables during 1st July (in number of hours from the start of the year) for the base case

OM 1 the wasted power gradually increases due to the increase of the TES outlet temperature when the thermocline is discharged. Similarly, during the second half of OM 3 the ST power decreases due to the partial thermocline discharge and the consequent TES outflow temperature drop.

For the year-round simulation, the net energy produced is 613.20 GWh_{e} , meanwhile the wasted thermal energy is 222.567 GWh_{th} (see data in Table 5). Specifically, the main component of the latter thermal energy wasted is represented by the remaining thermal power at the economizer hot side outlet. The higher the OM 1 share to the total hours, the better performance and design of the plant. According to results in Table 4, OM4 share should be reduced in order to increase CF. OM 1 share is higher than OM 2 and OM 3, so the initial design works for the whole year. With respect to CAPEX and OPEX, Fig. 4 shows the distribution of costs. For the capital investment, the field costs are the major ones, although plant installation and civil engineering represent together a big part of expenditure too. Meanwhile, in the OPEX case, the maintenance is the most expensive factor, followed by the fuel costs, since it includes costs associated with maintenance of the receiver and gas piping, mirror breakage, field control systems, ground keeping or mirror washing. In addition, expenses related to CO₂ emissions have been also taken into account and result to be the third ones in order of importance.

	TABLE 4. Operatin	g Modes shares for th	e annual simulation a	nd for the base case.	
ОМ	OM 1	OM 2	OM 3	OM 4	OM 5

Share (%)	18.32	6.36	10.01	45.36	19.96
TABLE 5. Net	annual energy and wa	asted energy for the sen	usitivity analysis. * Ba	use case for SM <u>. ** I</u>	Regular base case.
SM [-]	Net Energy [GWh _e]	Wasted Energy [GWh _{th}]	TES size [h]	Net Energy [GWh _e]	Wasted Energ [GWh _{th}]
1	546.588	174.584	4	593.407	290.395
1.25	665.725	199.976	6	602.012	240.264
1.5 *	788.224	225.444	8 **	613.197	222.567
1.75	906.222	249.712	10	618.680	219.668
2	1042.897	275.200	12	625.336	221.290
TCC [°C]	Net Energy [GWhe]	Wasted Energy [GWh _{th}]	γ[-]	Net Energy [GWhe]	Wasted Energ [GWhth]
800	436.762	308.384	3	643.873	266.750
900	433.823	215.020	5 **	613.197	222.567
1000	433.335	300.268	9	658.410	199.945
1100	501.952	324.685			
1200 **	613.197	222.567			
1300	723.407	361.302			
1400	838.168	383.061			

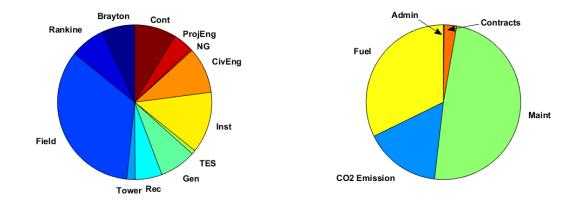


FIGURE 4. CAPEX (left) and OPEX (right) share for the base case

Sensitivity Analysis

The main results for the sensitivity analysis are reported in Fig. 5 and Table 5. The results show that an increase of TCC will lead to an increase of the Capacity Factor in the analyzed temperature range (Fig. 5 top left). Specifically, the CF remains almost constant for a TCC up to 1000°C, while for higher TCC a clear enhancement of the CF can be achieved. Thus, hybridization would be interesting for high TCC though this leads to higher CO₂ emissions. On the other hand, the LCoE trend displays a maximum for a TCC of 1000°C and a minimum for a TCC of 1300°C, showing that for assumed gas costs it is worth hybridizing the system. The variation of the TES size has a pretty clear relative influence on the final plant KPIs. With increasing TES size, the LCoE decreases, while the CF increases, as it was expected, and as it can observed in Fig. 5 (top right). This capacity factor increment is related also to a net energy rise. In addition, bigger TES leads to positive results in terms of reduction of wasted energy and CO₂ emissions. The results show that an increase of SM will lead to an increase of the Capacity Factor and a decrease of the LCoE in the analyzed range (Fig. 5 bottom left). As expected, a larger SM enables to store more energy in the TES during daytime and consequently to extend longer the power production during night, achieving higher CF. In this case, the improvement in the net electrical energy production is well enough to compensate for the increase in the required initial expenditure, leading to lower LCoE. A different trend can be identified considered the specific emissions, indeed a maximum is recorded for SM equal to 1.25, while for larger SM a decrease in the specific CO_2 emission is achieved. As a last input (Fig. 5 bottom right), increasing power ratio between the gas and steam cycle (γ) leads to higher specific emissions and CF. Indeed, a larger GT would require more fuel but it will also increase the power production during daytime.

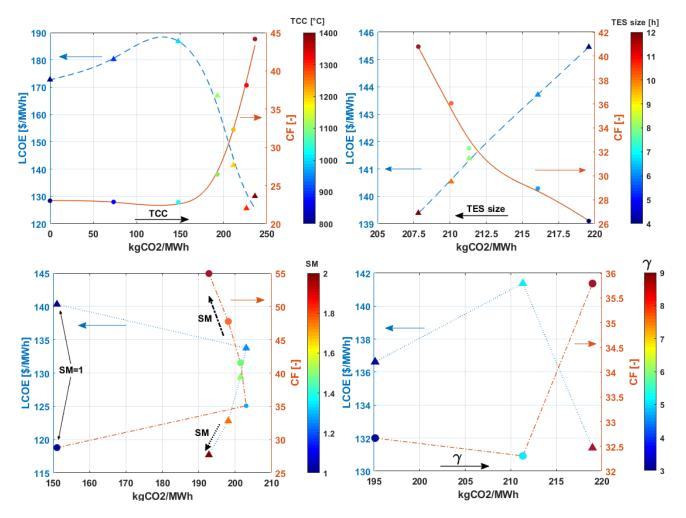


FIGURE 5. LCoE and Capacity Factor vs specific CO₂ emissions for a variable TCC (top left), for a variable TES size (top right), for a variable SM (bottom left), and for a variable GT-ST power ratio, γ (bottom right)

Instead a maximum trend can be recorded for the LCoE, indeed both studied GT to ST ratios enable lower LCoE and higher net energy production. The study shows that LCoE figures lower than 120 \$/MWh and capacity factors of about 55% can be achieved. Interestingly, the comparative analysis shown in Table 6 reveals that at such capacity factor the proposed configuration is only about two times more costly than an equivalent size CCGT, but at the same time yielding less than half of the emissions of the latter. Simultaneously, the proposed layout is considerably cheaper than an equivalent molten salt CSP plant. The analysis performed thus far reveals that the cycle is then worth continuing to explore, especially when considering the value of generation in time and when integrating a dispatch optimizer.

TABLE 6. Comparison between different electricity plants at 55% Capacity Factor.						
	Hybrid TES CSP	Molten salts CSP [6]	Conventional CCGT			
Emissions (kgCO ₂ /MWh)	192.78	0	464.91			
LCoE (\$/MWh)	117.69	137	54.01			

TABLE 6. Comparison between different electricity plants at 55% Capacity Factor

CONCLUSIONS

In this work a techno-economic assessment of an innovative solar-hybrid combined cycle has been performed. The studied plant is composed of a topping solar-hybrid gas turbine coupled to a bottoming packed bed thermal energy storage at the gas turbine exhaust, which runs in parallel also to a traditional bottoming steam cycle. In order to evaluate the plant performances, the following KPIs have been analyzed: capacity factor, specific CO_2 emissions, capital expenditure, and Levelised Cost of Electricity. The combustion chamber outlet temperature, solar multiple and energy storage capacity has been considered as decisional variables in the performed sensitivity analysis. The technoeconomic performance of the proposed plant has been compared against that of more conventional molten salt tower CSP plants and traditional combined cycle gas turbine power plants with equivalent installed capacities and load factors. The results show that capacity factor enhancement and consequent LCoE reduction would be enabled by high TCC, large TES size and large SM. Higher storage capacity and wider heliostat field seem to be a viable design choice as they lead to specific CO₂ emission reduction. Conversely, a trade-off can be identified between improvements in CF and LCoE and specific emissions while looking at the TCC. Moreover, for a capacity factor of about 55%, proposed plant configurations are associated with a Levelised Cost of Electricity lower than 120 \$/MWh. Under these working conditions, the suggested layout would be only about two times more costly than an equivalent size CCGT, although it will produce less than half of the emissions of the latter. At the same time, the proposed configuration is considerably cheaper than an equivalent molten salt CSP plant. Finally, the analysis performed thus far reveals that the cycle is worth continuing to explore, especially when considering the value of generation in time and when integrating a dispatch optimizer. Therefore, the authors would like to remark the value of decoupling the topping and bottoming cycles through an intermediate TES, which could be important in the framework of techno-economic optimization studies focused to flexible energy production and dispatch. Its capability even to account for hourly price variations or load profile demands is a suggesting work for the future.

ACKNOWLEDGMENTS

Financial support from University of Salamanca, Junta de Castilla y León of Spain under grant no. SA017P17, Banco Santander and Swedish Energy Agency and Azelio AB through the Energy Agency program Electricity from the Sun, project P43284-1 are acknowledged.

REFERENCES

- 1. P. J. Harper, T. W. Von Backström, T. P. Fluri and D. G. Kröger, "TRNSYS modeling of a 100 MWe hybrid combined cycle concentrating solar power plant", 1st Southern African Solar Energy Conference (SASEC, 2012).
- J. D. Spelling, "Hybrid Solar Gas-Turbine Power Plants. A Thermoeconomic Analysis", Ph.D. thesis, KTH Royal Institute of Technology, 2013. ISBN 978-91-7501-704-4.
- 3. Marshall Swift Valuation Services, "Report-Inventory Index Factors" (January 2018).
- J. B. Blackmon, Conc. Sol. Power Technol. Princ. Dev. Appl., 536–576 (2012). "Heliostat size optimization for central receiver solar power plants", doi:10.1016/B978-1-84569-769-3.50017-0.
- P. Schwarzbözl, R. Buck, C. Sugarmen, A. Ring, M. J. Marcos Crespo, P. Altwegg and J. Enrile, Sol. Energy 80, 1231-1240 (2005). "Solar gas turbine systems: Design, cost and perspectives", doi:10.1016/j.solener.2005.09.007.
 C. Turchi, M. Mebos, C. K. Ho and G. J. Kolb, "Current and Future Costs for Parabolic Trough and Power Systems in the
 - C. Turchi, M. Mebos, C. K. Ho and G. J. Kolb, "Current and Future Costs for Parabolic Trough and Power Systems in the US Market", presented at SolarPACES2010, (Perpignan, France, October 2010).